

The Virtual Photon Asymmetry A_2 and the Spin Dependent Structure Function xg_2 at HERMES

V.A. Korotkov^{*†}

Institute for High Energy Physics, Protvino, Russia

E-mail: Vladislav.Korotkov@ihep.ru

The HERMES experiment at DESY collected data on deep-inelastic scattering of 27.6 GeV longitudinally polarized leptons off transversely polarized hydrogen gas target internal to the HERA storage ring. The data were used to measure the proton spin structure function $g_2^p(x, Q^2)$ and the virtual photon asymmetry $A_2^p(x, Q^2)$ over the kinematic range $0.023 < x < 0.7$ and $1 < Q^2 < 15 \text{ GeV}^2$. The results are consistent, within experimental uncertainties, with expectations based on the Wandzura-Wilczek relation and with previous experimental data.

XVIII International Workshop on Deep-Inelastic Scattering and Related Subjects, DIS 2010

April 19-23, 2010

Firenze, Italy

^{*}Speaker.

[†]On behalf of the HERMES Collaboration.

The description of inclusive deep inelastic scattering of longitudinally polarized charged leptons off polarized nucleons requires two nucleon structure functions $g_1(x, Q^2)$ and $g_2(x, Q^2)$ in addition to the well-known unpolarized structure functions. Here, Q^2 is the negative squared four-momentum of the exchanged virtual photon with laboratory energy ν , $x = Q^2/2M\nu$ is the Bjorken scaling variable, and M is the nucleon mass. In the quark-parton model (QPM) the spin-dependent structure function $g_1(x, Q^2)$ describes the quark helicity distribution inside a longitudinally polarized nucleon. The spin-dependent structure function $g_2(x, Q^2)$ does not have a probabilistic interpretation in the QPM. Its properties have been established in the framework of the operator product expansion (OPE) analysis within nonperturbative QCD [1, 2]. Ignoring quark mass effects, $g_2(x, Q^2)$ can be written as a sum of two terms

$$g_2(x, Q^2) = g_2^{WW}(x, Q^2) + \bar{g}_2(x, Q^2). \quad (1)$$

Here, $g_2^{WW}(x, Q^2)$ is the twist-2 part derived by Wandzura and Wilczek [3]:

$$g_2^{WW}(x, Q^2) = -g_1(x, Q^2) + \int_x^1 g_1(y, Q^2) \frac{dy}{y}. \quad (2)$$

Second term, $\bar{g}_2(x, Q^2)$, is the genuine twist-3 part which measures quark-gluon correlations in the nucleon.

A measurement of the structure function $g_2(x)$ requires a longitudinally polarized beam and a transversally polarized target. The polarization-dependent part of the cross-section in this case is given by [4]:

$$\frac{d^3\Delta\sigma}{dx dy d\phi} = -h_l \cdot \cos\phi \frac{e^4}{4\pi^2 Q^2} \cdot \gamma \cdot \sqrt{1-y-\frac{\gamma^2 y^2}{4}} \left(\frac{y}{2} g_1(x, Q^2) + g_2(x, Q^2) \right). \quad (3)$$

Here, $h_l = \pm 1$ is the lepton helicity, e is the electron charge, $y = \nu/E$ is the fractional energy transferred to the nucleon, $\gamma = 2Mx/\sqrt{Q^2}$. The angle ϕ is the azimuthal angle about the beam direction between the lepton scattering plane and the ‘‘upwards’’ target spin direction. The contribution of the function g_2 to the polarized-dependent part of the cross-section is much smaller than the contribution of the function g_1 and, as a result, the functions g_2 and A_2 have been measured [5, 6, 7] with a comparatively poor accuracy only. This paper reports a new measurement of g_2 and A_2 . The data were collected during the 2003 – 2005 running years with the HERMES spectrometer [8] using a transversely nuclear-polarized gaseous hydrogen target [9] internal to the $E = 27.6$ GeV HERA storage ring at DESY. The open-ended target cell was fed by an atomic-beam source based on Stern-Gerlach separation combined with radio-frequency transitions of hydrogen hyperfine states. The nuclear polarization of the atoms was flipped at 1-3 minute time intervals, while both the polarization magnitude and the atomic fraction inside the target cell were continuously measured. The average value of the proton polarization was 0.78 ± 0.04 . Tracking corrections were applied for the deflections of the scattered leptons caused by the vertical 0.3 T target holding field, with a small effect on the extracted asymmetries. The lepton beam (positrons during 2003-2004 data-taking years and electrons in 2005) was self-polarized in the transverse direction due to the Sokolov-Ternov effect [10]. Longitudinal orientation of the beam spin was obtained by using a pair of spin rotators located before and behind the interaction region of HERMES spectrometer. The beam helicity

was flipped every few months. The beam polarization was measured by two independent HERA polarimeters [11]. The average value of the polarization was found to be 0.34 ± 0.01 . The scattered leptons were detected by the HERMES spectrometer within an angular acceptance of ± 170 mrad horizontally and $\pm(40 \div 140)$ mrad vertically. The leptons were identified using the information from an electromagnetic calorimeter, a transition-radiation detector, a preshower scintillating counter and a dual-radiator ring imaging Čerenkov detector [12]. The identification efficiency for leptons with momentum greater than 2.5 GeV/c exceeds 98%, while the hadron contamination is found to be less than 1%. The luminosity monitor [13] measured e^+e^- pairs from Bhabha (Møller in case of electron beam) scattering off the target gas electrons, and $\gamma\gamma$ pairs from e^+e^- annihilation in two NaBi(WO₄)₂ electromagnetic calorimeters, which were mounted symmetrically on either side of the beam line.

The polarization-dependent part of the cross-section (3) exhibits a $\cos \phi$ azimuthal asymmetry, which experimentally can be measured in the following way:

$$A_{\perp}(x, Q^2, \phi) = \frac{N^-L^+ - N^+L^-}{N^-L_p^+ - N^+L_p^-}. \quad (4)$$

Here, $N^{+(-)}$ is the number of scattered leptons in one bin of the 3-dimensional space (x, Q^2, ϕ) for a case when the proton spin is up(down). $L^{+(-)}$ and $L_p^{+(-)}$ are the corresponding luminosities and the luminosities being weighted with absolute value of the beam and target polarization product, respectively. Asymmetries (4) were measured for each of the two beam helicities, found to be consistent, and then properly averaged.

The kinematic requirements imposed on the data were: $1 < Q^2 < 15 \text{ GeV}^2$, invariant mass of the virtual photon-nucleon system $W > 2 \text{ GeV}$, $0.023 < x < 0.7$, $0.1 < y < 0.85$. Applying data quality criteria resulted in about seven million events available for the asymmetry analysis. The kinematic region covered by the experiment in (x, Q^2) space was divided into six bins in x and into three logarithmically equidistant bins in Q^2 . The purpose of the binning in Q^2 is to decrease the error inflation of the results due to the unfolding procedure (see below). The whole range in ϕ -space $(-\pi \div \pi)$ was divided into 10 bins. Two of the ϕ -bins cover the shielding steel-plate region of the spectrometer and thus cannot be used for the analysis. The data were corrected for the e^+e^- charge symmetric background, which amounts in total to about 1.8% of the statistics. Finally, the asymmetry (4) was unfolded for radiative higher order QED and instrumental smearing effects to obtain the asymmetry corresponding to pure single-photon exchange in the scattering process. The unfolding procedure is analogous to that used in the analysis of the structure function $g_1(x, Q^2)$ [14].

According to formula (3) the asymmetry (4) linearly depends on $\cos \phi$, i.e.:

$$A_{\perp}(x, Q^2, \phi) = A_T(x, Q^2) \cdot \cos \phi.$$

The asymmetry amplitude $A_T(x, Q^2)$ is obtained by fitting the unfolded asymmetries (4) with the function $f(\phi) = A_T(x, Q^2) \cdot \cos \phi$. Finally, the functions $g_2(x, Q^2)$ and $A_2(x, Q^2)$ were evaluated from the amplitude A_T and the previously measured function g_1 (a parameterization of g_1 [15] was used) through the following relations:

$$g_2 = \frac{F_1}{\gamma d(1 + \gamma\xi)} A_T - \frac{F_1(\gamma - \xi)}{\gamma(1 + \gamma\xi)} \frac{g_1}{F_1}, \quad (5)$$

$$A_2 = \frac{1}{d(1+\gamma\xi)} A_T + \frac{\xi(1+\gamma^2)}{1+\gamma\xi} \frac{g_1}{F_1}. \quad (6)$$

Here, $d = D\sqrt{1-y-\gamma^2y^2/4}/(1-y/2)$, $\xi = \gamma(1-y/2)/(1+\gamma^2y/2)$, and D is the fraction of the beam polarization transferred to the virtual photon:

$$D = y(2-y)(1+\gamma^2y/2)/[y^2(1+\gamma^2) + 2(1-y-\gamma^2y^2/4)(1+R)].$$

The unpolarized structure function $F_1(x, Q^2)$ was calculated using a parameterization of the unpolarized structure function $F_2(x, Q^2)$ [16] and the ratio of longitudinal to transverse virtual-photon absorption cross sections $R(x, Q^2)$ [17], $F_1 = F_2(1+\gamma^2)/[2x(1+R)]$. All kinematic factors in relations (5)-(6) and the functions F_1 and g_1/F_1 were calculated at average values of x and Q^2 in each $x - Q^2$ bin at the Born level.

The final result for each of the x bins is the weighted average [14] of the results obtained in the corresponding three Q^2 bins. Before averaging, the results of measurements in each of the Q^2 bins must be evolved to a common value of $Q^2 = Q_{avg}^2$, which is the mean Q^2 for a particular x bin. The evolution of function $A_2(x, Q^2)$ was done assuming that $\sqrt{Q^2}A_2$ does not depend on Q^2 . The structure function $g_2(x, Q^2)$ was evolved assuming that its Q^2 dependence is analogous to that for the Wandzura-Wilczek part of g_2 . This produces a very small effect because g_2 depends on Q^2 only weakly and the level arm over Q^2 is relatively small.

The dominant sources of systematic uncertainties in this study are the uncertainties on beam and target polarization values which in total produces a 10% scale uncertainty on the value of A_2 and xg_2 . Other sources of systematic uncertainties such as the acceptance effects, a possible target polarization misalignment, the unfolding procedure and a possible correlation between prefactors of the A_T and the A_T itself in relations (5)-(6) were evaluated by Monte Carlo studies. Uncertainties stemming from parameterizations of $g_1(x, Q^2)$, $F_2(x, Q^2)$ and $R(x, Q^2)$ were estimated also. The total systematic uncertainty, except the scale uncertainty due to the beam and target polarization measurements, was evaluated as a sum in quadrature of all the considered sources. Its magnitude is several times less than statistical uncertainty.

Final results on the virtual photon asymmetry $A_2(x)$ and the spin-dependent structure function $xg_2(x)$ are presented in Fig. 1 on the left and right panels, respectively. One should note that the unfolding procedure leads to the statistical correlations between results in different kinematic bins. Statistical uncertainties presented in Fig. 1 correspond to the diagonal elements of the covariance matrix obtained from the unfolding algorithm. Data from experiments E155 [7], E143 [6], and SMC [5] are shown as well. The experiments have slightly different values of average Q^2 for a particular value of x . The solid curves represent values of $A_2(x)$ and $xg_2(x)$ evaluated with the Wandzura-Wilczek relation (2) at Q^2 values of HERMES data.

In conclusion, HERMES measured the spin structure function $g_2^p(x)$ of the proton and virtual photon asymmetry $A_2^p(x)$ in the kinematic range $0.023 < x < 0.7$ and $1 < Q^2 < 15 \text{ GeV}^2$. The results are in agreement, within experimental uncertainties, with those obtained in experiments E155 [7], E143 [6], and SMC [5] and with calculations accounting the twist-2 part of $g_2(x, Q^2)$ only.

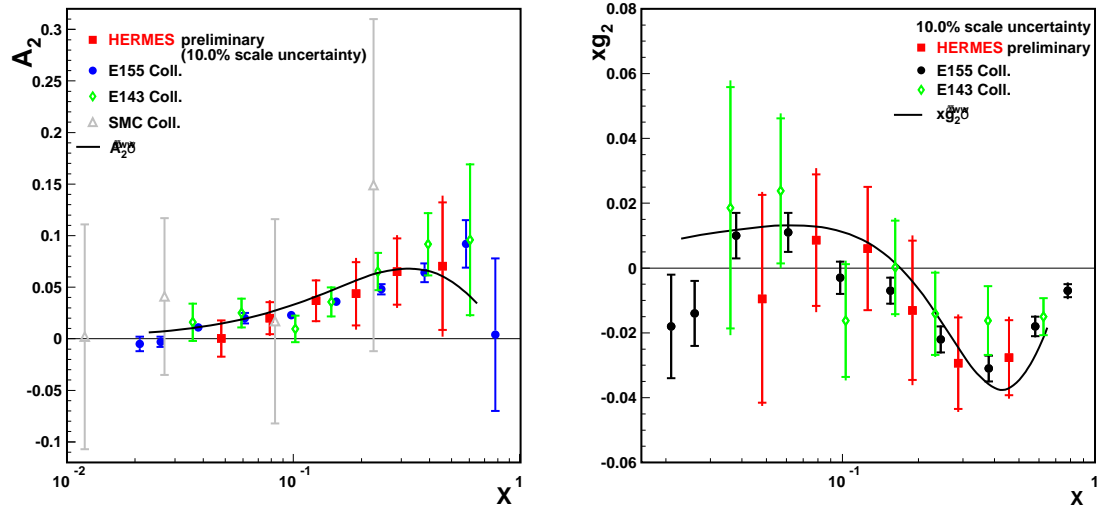


Figure 1: Left panel: The virtual photon asymmetry A_2^p as a function of x . Right panel: The spin structure function xg_2^p as a function of x . HERMES data are shown together with data from E155 [7], E143 [6], and SMC [5] experiments. Full error bars for this study represent the sum in quadrature of statistical and systematic uncertainties. The statistical uncertainties are shown by the inner error bars. The solid curve is the prediction following from Wandzura-Wilczek relation (2).

References

- [1] E.V. Shuryak and A.I. Vainshtein, *Nucl. Phys. B* **201**, (1982) 141.
- [2] R.L. Jaffe and X.J. Ji, *Phys. Rev. D* **43**, (1991) 724.
- [3] S. Wandzura and F. Wilczek, *Phys. Lett. B* **72**, (1977) 195.
- [4] R.L. Jaffe, *Comments Nucl. Part. Phys.* **19**, (1990) 239.
- [5] SMC Coll., D. Adams *et al.*, *Phys. Rev. D* **56**, (1997) 5330.
- [6] E143 Coll., K. Abe *et al.*, *Phys. Rev. D* **58**, (1998) 112003.
- [7] E155 Coll., P.L. Anthony *et al.*, *Phys. Lett. B* **553**, (2003) 18.
- [8] K. Ackerstaff *et al.*, *Nucl. Instrum. Methods A* **417**, (1998) 230.
- [9] A. Airapetian *et al.*, *Nucl. Instrum. Methods A* **540**, (2005) 68.
- [10] A.A. Sokolov, I.M. Ternov, *Sov. Phys. Doklady* **8**, (1964) 1203.
- [11] M. Beckmann *et al.*, *Nucl. Instrum. Methods A* **479**, (2002) 334.
- [12] N. Akopov *et al.*, *Nucl. Instrum. Methods A* **479**, (2002) 511.
- [13] T. Benisch *et al.*, *Nucl. Instrum. Methods A* **471**, (2001) 314.
- [14] HERMES Coll., A. Airapetian *et al.*, *Phys. Rev. D* **75**, (2007) 012007.
- [15] E155 Coll., P.L. Anthony *et al.*, *Phys. Lett. B* **493**, (2000) 19.
- [16] D. Gabbert and L. De Nardo (2007), ArXiv:hep-ph/0708.3196.
- [17] E143 Coll., K. Abe *et al.*, *Phys. Lett. B* **452**, (1999) 194.